On the electrical degradation and green band formation in α- and β-phase poly(9,9-dioctyfluorene) polymer light-emitting diodes

B. Arredondo [a,*], B. Romero [a], A. Gutiérrez-Llorente [a], A.I. Martínez [a], A.L. Álvarez [a], X. Quintana [b], J.M. Otón [b]

[a] Dpto. Tecnología Electrónica, Universidad Rey Juan Carlos, C/Tulipán s/n, 28933, Móstoles, Madrid, Spain
[b] Dpto. Tecnología Fotónica, Universidad Politécnica de Madrid, Ciudad Universitaria s/n, 28040 Madrid, Spain

Keywords:
Polymer light-emitting diodes
Polyfluorene
β-Phase
Degradation

A B S T R A C T

In this work we report a detailed comparison of optical and electrical degradation between α- and β-phase poly(9,9-dioctyfluorene) (PFO) based diodes. Analysis of the EL spectra along continuous operation time in α- and β-PFO based diodes reveals that the unwanted green emission traditionally associated to fluorenone is more likely to occur in α-phase PFO. The relative spectral areas arising from excitonic and vibronic transitions as well as fluorenone defects have been quantified by means of Gaussian deconvolution along the operation time. The relative spectral area associated to the formation of the fluorenone increases 13% for the β-PFO diode and up to 21% for the α-PFO diode only after 35 min of continuous operation. Analysis of the *I–V* curve before and after electrical stressing has lead to hole mobilities in pristine diodes of 1.4×10^{-4} cm^2/Vs and 1.6×10^{-5} cm^2/Vs for β-PFO and α-PFO respectively. Both β-PFO and α-PFO degraded samples show a reduction in the hole mobility, as well as an increase in the width of the Gaussian density of states.

1. Introduction

Polyfluorenes (PFs) have been widely studied due to their interesting properties as blue emitters for solution-processable polymer light-emitting diodes (PLEDs). PFs are soluble in conventional organic solvents such as aromatic hydrocarbons (Toluene, Tetrahydrofuran (THF), etc.) and chlorinated hydrocarbons (i.e. Chloroform) and result in high quality thin films when processed by spin coating. PLEDs based on PF exhibit high efficiencies, reasonable mobilities and good thermal and chemical stability [1,2]. One of the most attractive PFs is poly(9,9-dioctyfluorene) (PFO). Its interest resides not only in its technological potential for various optoelectronic applications, but also from the material structure point of view, in the different phases it shows [3,4]. In this sense, PFO can be prepared in a range of morphological phases [5,6]. Two well-known different conformations adopted by PFO are an amorphous α-phase and a highly ordered phase, termed the β-phase. This β-phase is composed of polymer backbones with a more planar configuration which extends the mean conjugation length [7]. This new conformation results in an increase of electronic delocalization which in turns leads to a red-shifted absorption and emission bands [7,8]. The β-phase is thoroughly studied due to its greater colour stability at high bias and its high photoluminescence quantum efficiency [3,9]. β-Phase always appears as a minority constituent in the absorption but the optical emission is dominated by β-type contributions, even for a small amount (less than 10%) of β-phase embedded in a disordered glassy (α-phase) matrix [10,11]. Therefore, optical performance of a PFO based device depends enormously on the β-phase amount of the active layer. Improved PLED performance with low contents of β-phase has been attributed to efficient energy transfer and charge trapping, which leads to a better balance of charges and more efficient exciton formation [4,12]. While the exact mechanism of β-phase formation is still not well understood, numerous methods have been carried out to alter the morphology of PFO and control the formation of this phase. These approaches include thermal cycling (cooling and slow reheating at room temperature) and exposure to certain solvent vapour of spin-coated glassy thin films [4,13–15], incorporation of high boiling point additives into the solvent [7,12,16] and the use of concentrated solutions, poor solvents and low temperatures [6,17,18]. It has also been speculated that the appearance of β-phase might be related to a low solvent evaporation rate. Some authors have achieved this mechanically by introducing the samples in a box with a small aperture and controlling the temperature [3].

Most of the above mentioned studies in β-phase are focused on the different ways to obtain such a phase in film and its morphological and photophysical characterization. Besides, few works report on a device structure exhibiting β-phase and characterized the final diode in terms of luminance at different voltages or current bias [3,4,9,16]. Moreover, to our knowledge, no study has been carried out to assess colour stability with current and with continuous

* Corresponding author. Tel.: +34 (91) 4888238; fax: +34 (91) 6647049.
E-mail address: belen.arredondo@urjc.es (B. Arredondo).

0038-1101/$ - see front matter © 2011 Elsevier Ltd. All rights reserved.
doi:10.1016/j.sse.2011.02.004

operation time of β-phase PFO based diodes. Futhermore, it appears interesting to analyze the *I–V* curves of α-phase and β-phase PFO based diodes using theoretical conduction models in order to obtain differences in the material properties such as carrier mobility which in turn will determine the device electrical behaviour.

In this work we fabricated α-phase and β-phase PFO based diodes and compare the colour stability of both devices at different bias and for different times of continuous operation. Active layers of all devices were deposited by spin coating from a toluene based solution, controlling the solution and the annealing temperature. The colour stability was studied by analyzing the electroluminescence spectra (EL) by means of Gaussian deconvolution. *I–V* curves have been analyzed before and after sample degradation by fitting the data to a theoretical model. This procedure leads to material and structure parameters such as hole mobility (μ), injection barrier (Δ) and width of Gaussian density of states (σ).

2. Experiment

The entire fabrication process is carried out in a clean room (class 10,000). Commercial indium–tin–oxide (ITO, thickness = 100 ± 5 nm) coated glass is used as substrate. Prior to film deposition, substrates went through a typical organic material cleaning process. Poly(3,4-ethylenedioxythiophene)/poly(4-styrenesulfonate) (PEDOT:PSS) was used as hole transport layer. The fabrication process consists of several steps. First, ITO coated glass is patterned by means of a photolithographic process. All layers are deposited in a glove box under N_2 atmosphere. PEDOT:PSS is spin-coated at 6000 rpm and dried at 100 °C for 30 min. Active layers are spin-coated at 6000 rpm from two different solutions with nominal equal concentration of 1% wt in toluene. Samples were deposited and cured at different temperatures, in order to control the β-phase formation. β-phase films were obtained when curing the samples at 70 °C in oven. This temperature is well below toluene boiling point (110 °C), ensuring a slow evaporation rate. On the other hand, when films were annealed at 100 °C in a hot plate, β-phase does not appear, and thus, samples only show α-phase. It has been observed that different annealing treatments of both devices, together with small differences in solution concentration of α and β-PFO films, may be the cause of the differences in the active layer thickness, being 30 nm for the α-PFO and 50 nm for β-PFO. Finally the Ba–Al cathode is thermally evaporated on top of the organic layer surface in a 10^{-6} Torr atmosphere. Including a thin layer of barium (~20 nm) at the cathode helps electron injection and hence diminishes threshold voltage. Finally, devices are encapsulated using a glass cover attached by a bead of epoxy adhesive. The final device has a structure: ITO/PEDOT:PSS/PFO/Ba–Al. The diode active area for α-devices was 2 mm^2 and for β-devices was 8 mm^2. Two types of devices with active layers α-PFO phase and β-PFO phase were studied. Biasing is provided through an ITO path that connects each contact to the outer wire. A detailed description of the fabrication procedure is found in previous works [19,20].

Current–voltage (*I–V*) characteristics were recorded using an Agilent 4155C semiconductor parameter analyzer and an Agilent 41501B SMU pulse generator. Samples were voltage driven under dc conditions. Luminance and EL spectra were recorded using a CS-1000 Minolta Spectroradiometer. Samples were current driven under dc conditions. Absorption spectra of thin PFO films were measured using a UV–VIS–NIR Spectrophotometer Varian Cary Scan 500.

3. Results and discussion

Films of α-PFO and β-PFO were prepared by spin coating in glass substrates following the same time and temperature annealing conditions as in PFO diodes. Films were examined by absorption spectroscopy, taking into account the absorption of glass and subtracting it to the sample absorption spectra. Fig. 1a shows the normalized absorption spectra of the α-PFO and β-PFO, taken at room temperature. Both absorption spectra show a main peak at around 380 nm, corresponding to the standard morphology of α-phase. Moreover, the β-phase spectrum shows an additional peak at 433 nm, typically assigned to the β-phase. This implies that in fact, in the so-called β-PFO film, there is a co-existence of both α- and β-phases. It is possible to take advantage of the differences in the absorption spectra to estimate the amount of β-phase by subtracting the contribution of the amorphous PFO [2,8]. This method consists of normalizing the absorption spectrum of α-PFO and β-PFO films. Subtraction of the α-PFO normalized curve from the normalized β-PFO spectrum yields the relative absorption of the β-phase and thus the total percentage of β-phase in the film can be estimated [7,8]. Fig. 1b shows the calculated β-phase absorption spectrum following the above procedure. The calculated total amount of β-phase is 9%.

Fig. 2a and b show the luminance vs the driving current for the α-PFO and β-PFO based PLED respectively. Insets show *I–V* curve for both diodes. It can be seen that the threshold voltage, Vth (defined as the required voltage to begin conduction above the shoulder) is slightly higher for the β-PFO based PLED, around 4.5 V, while this value is approximately 3.5 V for the α-PFO based PLED. This difference in Vth is attributed to a disparity in active layer thicknesses, being 30 nm for the α-PFO and 50 nm for the β-PFO.

Several works on colour stability in β-phase devices report EL measurements at different voltages to study optical degradation [3]. However, as mentioned before, PLEDs are current driven and one should also take into account that electrical degradation may also take place, meaning that at a constant voltage, the current diminishes causing a reduction in EL intensity (and hence luminance) [19]. This electrical degradation may hinder any significant change in the spectral shape. In this work, current

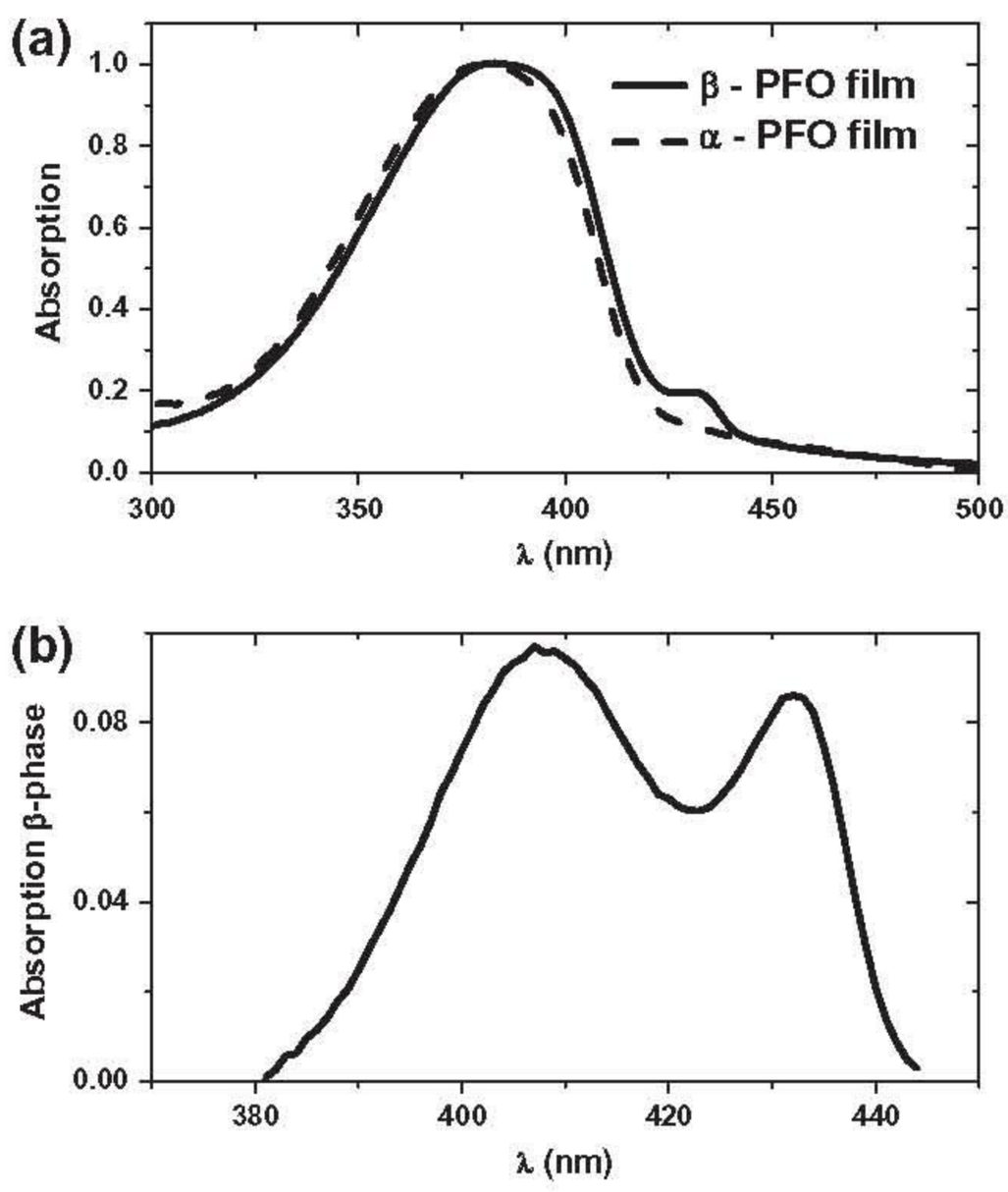

Fig. 1. (a) Normalized absorption of β-PFO and α-PFO films. (b) Calculated β-phase absorption spectrum based on subtraction of the α-PFO absorption.

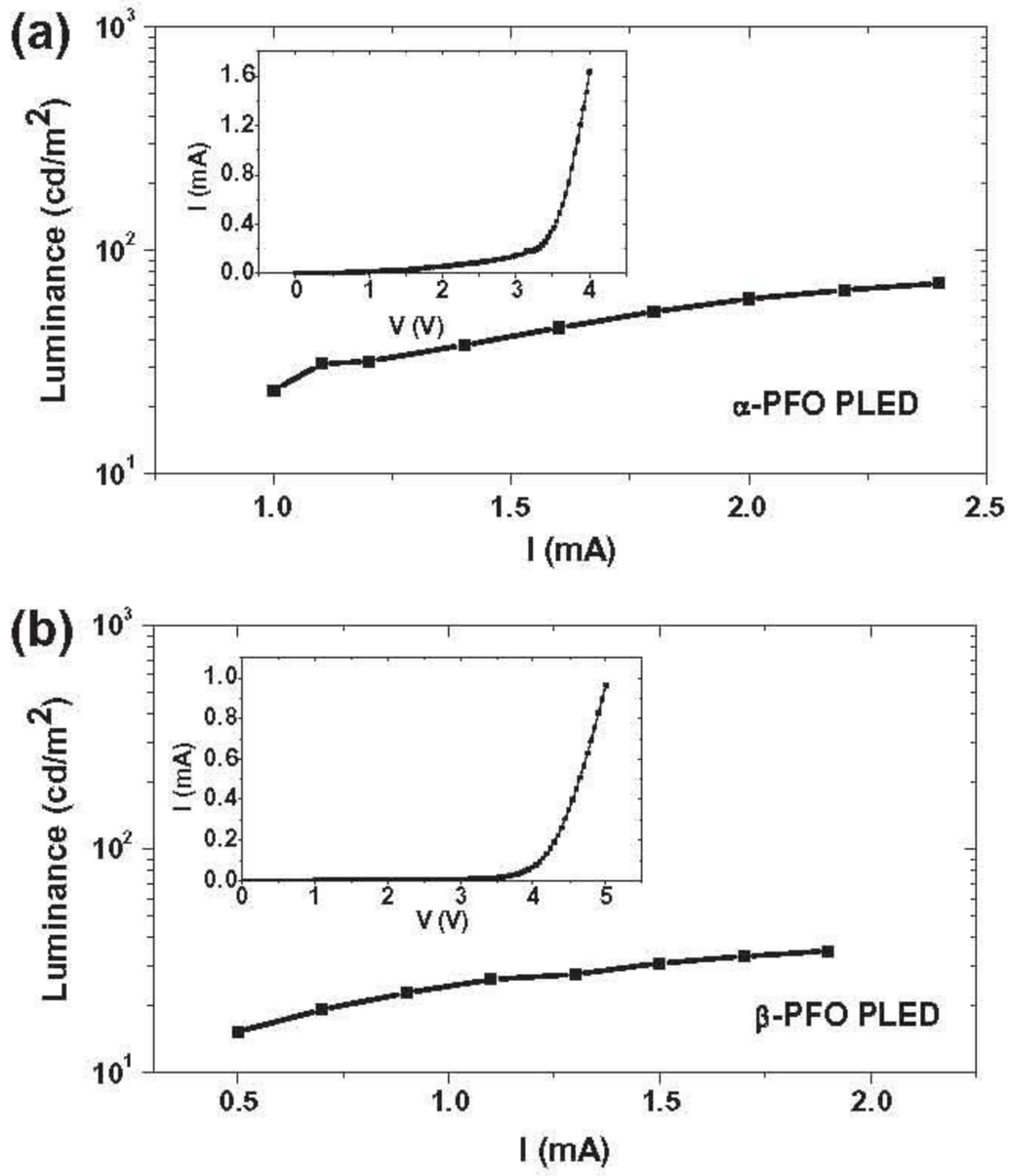

Fig. 2. (a) Luminance vs bias current for the α-PFO based PLED (b) Luminance vs current bias for the β-PFO based PLED. Insets show the corresponding *I–V* curves.

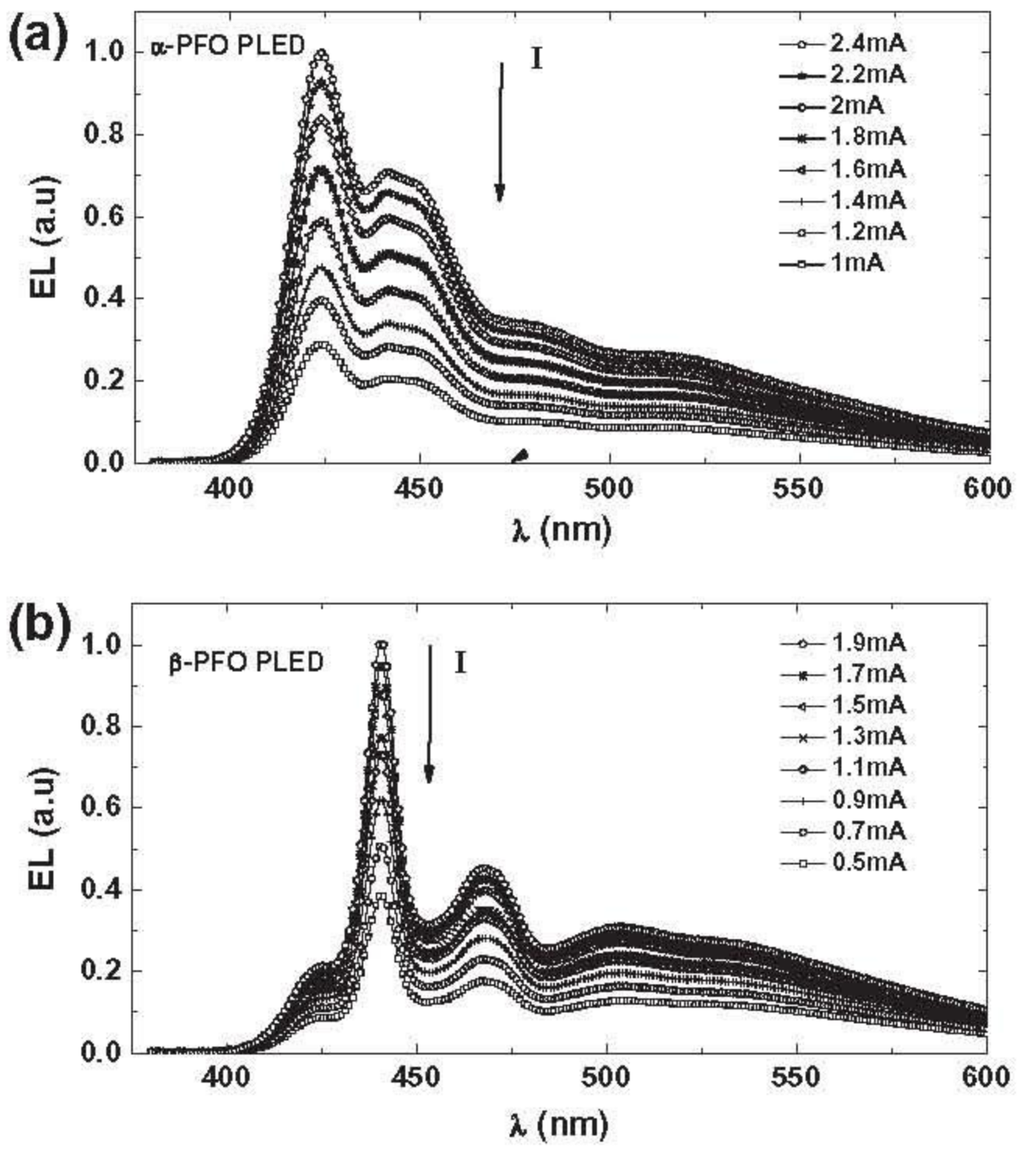

Fig. 3. Normalized EL spectra at different bias currents for the α-PFO PLED (a) and β-PFO PLED (b). EL spectra were normalized to the maximum value of the highest curve in order to observe the EL decay.

was kept constant in order to study the colour stability and device optical degradation. EL spectra were recorded at different current bias for both diodes (the voltage was adjusted in order to maintain a constant current).

Fig. 3a shows typical spectra for a α-PFO based PLED. The spectra are mainly composed by a peak at 423 nm corresponding to the excitonic transition (0–0 band), a vibronic peak at 446 nm (0–1 band) and two additional secondary features at 477 nm and 526 nm. The peak at 477 nm is attributed to a second vibronic replica (0–2 band), supported by the coincidence in the energy shift (around 170 meV). The feature at 526 nm has been widely studied and is attributed to the formation of fluorenone in the presence of oxygen or so called keto defect [21–25]. Keto defects are explained as the incorporation of oxygen as C=O bonds in the polymer backbone. They can be formed during synthesis or as a result of electro- (or photo) oxidative generation process of almost any PFs and result in an undesired green emission band. Besides, several studies show that some polyfluorene derivatives exhibit a feature at 470–500 nm as a result of electrooxidation with increasing bias current causing the appearance of a new chemical spice [19,26]. However, in the case of PFO there is no experimental evidence of such a phenomenon, in fact, the normalized spectra show that the 477 nm peak diminishes as bias current increases, reinforcing the hypothesis of a second order vibronic. Fig. 3b depicts the EL spectra of the β-PFO PLED. Well resolved red shifted peaks at 440 nm (0–0 β-phase band) and 463 nm (0–1 β-phase band) are observed, indicating that the spectral characteristics are completely dominated by the amount of β-phase present in the devices, and are red-shifted from those found in diodes based on amorphous PFO. Besides, a minor shoulder at 422 nm appears associated to the excitonic transition of the α-phase, and a broadband centred at about 511–530 nm associated to the keto defect. It is worth mentioning that this latter peak is very unlikely to respond to a second vibronic replica of the β-phase since the energy difference (around 250 meV) greatly exceeds that between the main transition and second order vibronic (approx. 150 meV). The minor contribution of the α-phase to the EL spectra of Fig. 3b implies, on one hand, a fast and effective energy transfer from the α- to the β-phase domains. On the other hand, because of the smaller energy gap of the β-phase compared to the energy gap of the α-phase, β-phase may act as low-energy traps for both singlet and triplet excitons. Both, the exciton migration from α- to β-domains, and the fact that β-phase can behave as trapping centres results in a minor contribution of the α-phase to the EL spectra even for films containing only a small fraction of β-phase.

A careful look at the spectra reveals that the contribution of each peak to the total emission is maintained constant as current is increased for both devices, α-PFO and β-PFO diodes. This is confirmed by the CIE coordinates, that maintain constant values with current, (0.20, 0.20) for the α-PFO PLED and (0.21, 0.22) for the β-PFO PLED, indicating good colour stability and no degradation effects. The higher value of the CIE coordinates for the β-PFO PLED results from the red-shifted EL spectra. These measurements were taken instantly using pristine diodes to avoid the influence of time degradation. It should be noticed that in samples with thin active layers the device efficiency could be affected by the quenching effects of PEDOT:PSS and the metal cathode. However, in terms of EL spectra, previous works show that thin films favours the appearance of a peak centred at around 470–510 nm due to the electron accumulation at the PEDOT:PSS interface [19]. This wavelength region is well above the α- and β-phase main transitions.

Fig. 4 shows the evolution of the EL spectra recorded along 35 min of continuous dc operation at 500 μA for the β-PFO diode (a) and 100 μA for the α-PFO diode (b). These are very conservative bias current conditions so that if degradation occurs is mainly due to cyclic operation. These driving currents have been chosen so that the initial luminance in both devices were similar, 15 cd/m^2 and 22 cd/m^2 for β- and α-phase devices respectively. As expected, the EL intensity diminishes with time for both diodes indicating

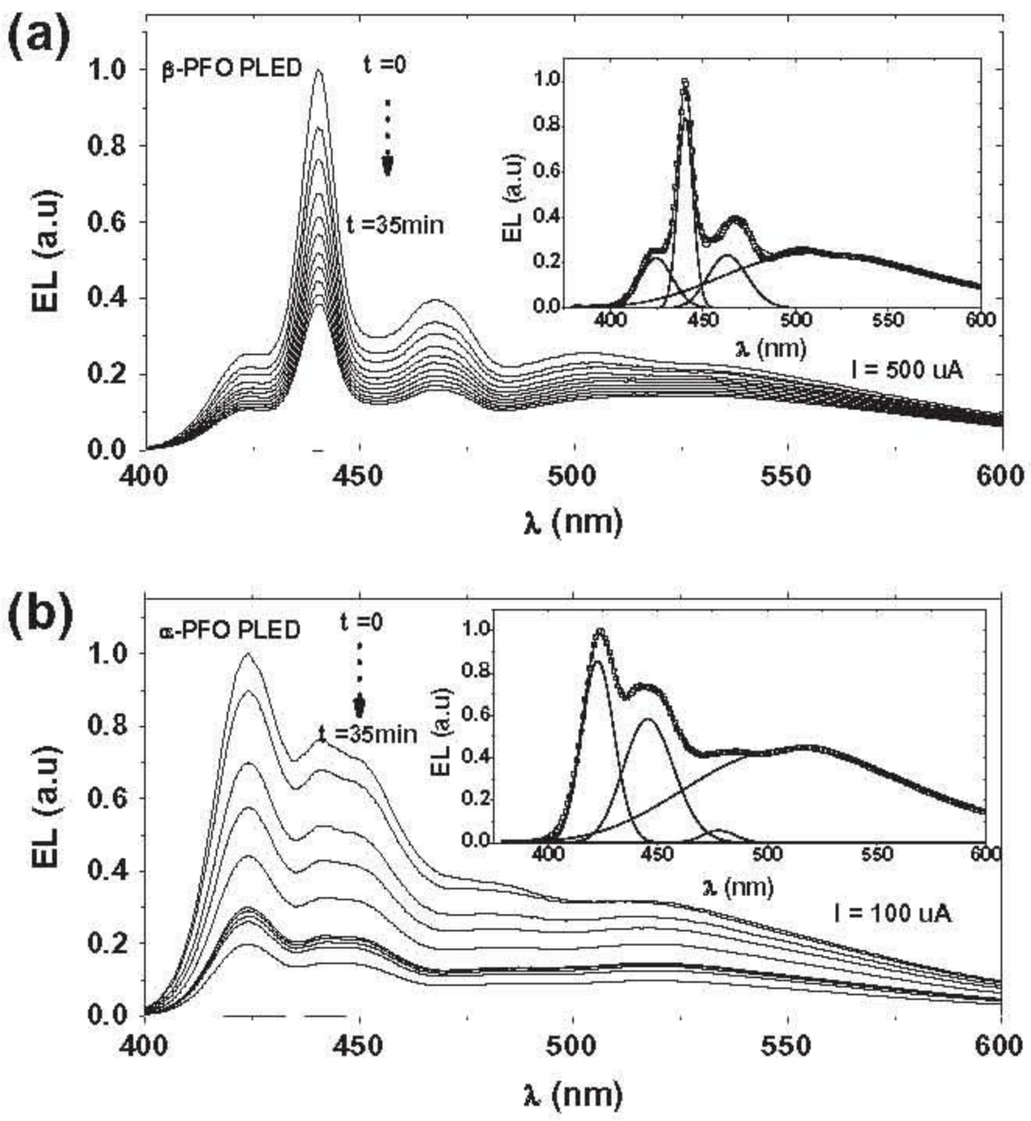

Fig. 4. Normalized EL spectra evolution for 35 min of continuous operation under dc conditions for the β-PFO PLED (a) and α-PFO PLED (b). Insets show the Gaussian deconvolution for one EL spectra after 15 min of continuous dc operation. Deconvolutions were performed in the energy domain, although they are shown as function of wavelength. EL spectra were normalized to the maximum value of the highest curve in order to observe the EL decay.

that luminance is also decreasing, 37% for the β-PFO diode and 69% for the α-PFO diode, see Fig. 5.

However, the fact that luminance decays does not indicate by itself that optical degradation is taking place, understood as an energy transfer from the main transitions (0–0 band and 0–1 band) to the fluorenone sites. Luminance decrease is most probable due to an electrical degradation, meaning the need to increase bias current in order to maintain a constant level of light emission. A quick look at the spectra may suggest that relative contribution of all peaks may remain constant in both diodes. Nevertheless, a careful analysis reveals an increase of the green component in the total spectral emission, this being significantly more pronounced for

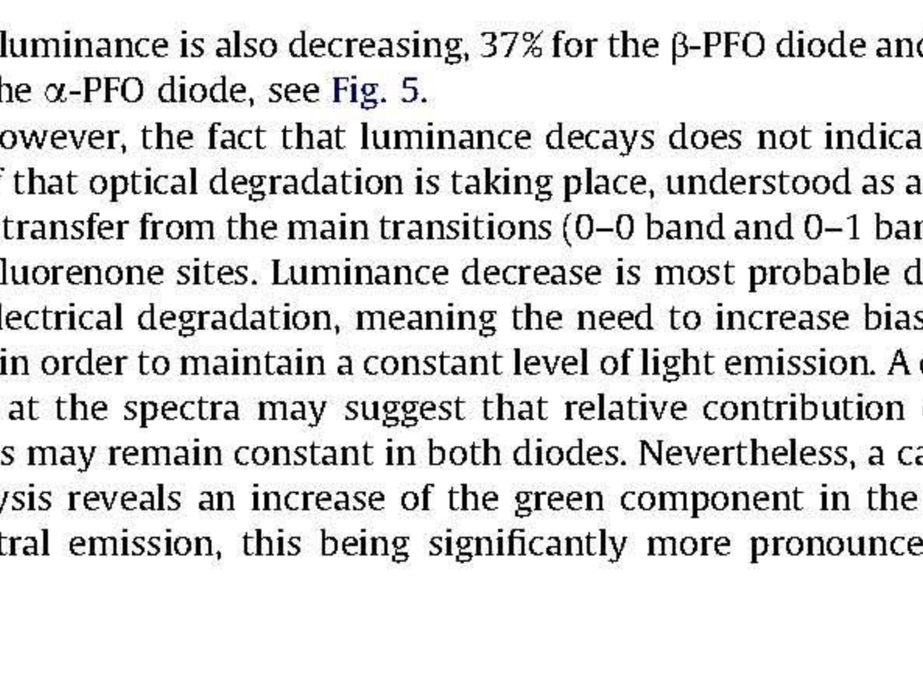

Fig. 5. Luminance decay versus time at a constant current: 500 μA for the β-PFO PLED and 100 μA for the α-PFO PLED. Luminance values are normalized to the initial values of pristine devices.

the α-PFO PLED. EL spectra were decomposed by means of Gaussian analysis to investigate the contribution of each peak to the total emission. Insets in Fig. 4 show two examples of Gaussian deconvolution after 15 min of continuous operation. Four Gaussians are used, each one centred at one of the significant peaks of the EL spectra. It should be pointed out that although spectra are plotted as a function of wavelength, Gaussian deconvolution was performed in the energy domain. In the case of β-phase devices, EL spectrum shows one main peak at 530 nm and a minor peak at 510 nm. This latter peak could correspond to the second order vibronic of the β-phase main transition. However, the contribution of this area is small compared to the keto one, and hence, both peaks have been modelled using one Gaussian in order to simplify the calculation and maintain the same number of Gaussians in both devices. It should be noticed that the α-phase contribution in Fig. 4a is more than the main peak at 420 nm. Transitions associated to β-phase screen those of α-phase, since they occur at similar energies. In particular, the main β-phase transition is very close to the first vibronic of the α-phase, and hence the effect of lattice phonons associated to the α conformation is hindered by the main β-phase band. Fig. 6 shows the relative spectral area associated to every peak versus time for β-PFO PLED (a) and α-PFO PLED (b). It is remarkable that in both devices the keto contribution to the spectra is above 50% of the total EL area. This initial high keto contribution can be attributed to the oxidation process during active layer thermal annealing. Although devices were fabricated under N_2 atmosphere, the solution preparation was carried out outside the glovebox. This favours the incorporation of oxygen in the active layer. It should be noticed that while the peaks related to both, α- and β-phase 0–0 band slightly decrease, the main difference is observed in the contribution of the relative spectral area associated to the fluorenone or keto defect. The contribution of the fluorenone to the total emission only after 35 min of continuous operation increases 13% for the β-PFO diode and up to 21% for the α-PFO diode. Since both devices are based on the same material lot and using the

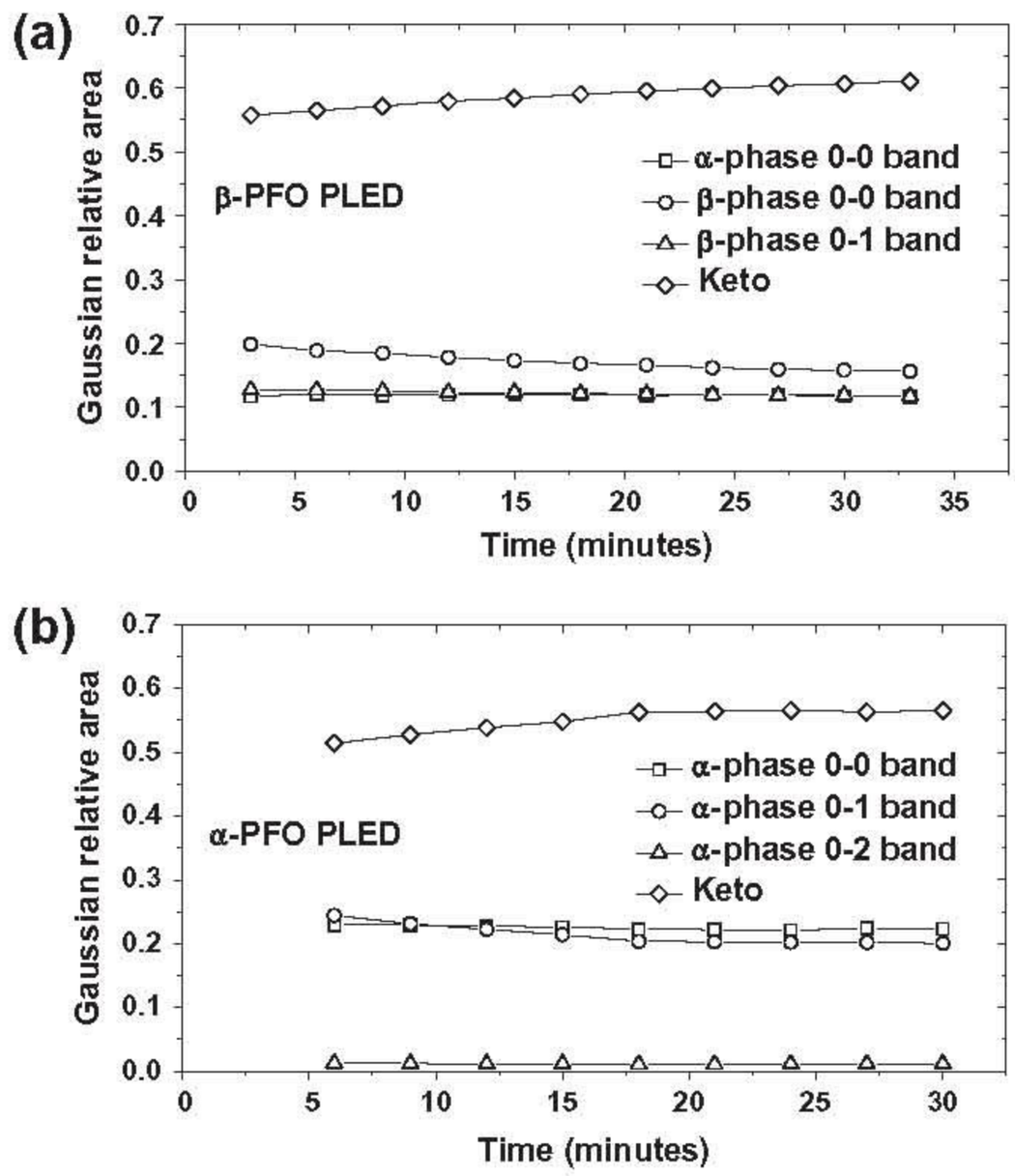

Fig. 6. Sum of the relative areas of the Gaussians curves associated to each peak versus time: β-PFO PLED (a) and α-PFO PLED (b).

same solvent, and were fabricated and measured under the same conditions, two causes for this difference can be inferred: (i) either that the β-phase is more stable and less reactive to oxygen, and thus the formation of the keto upon reaction of oxygen in the C-9 carbon is less probable, (ii) or that energy transfer from the main transition bands to the fluorenone sites are less likely to occur in β-PFO phase. Recent studies propose that the unwanted green emission is more related to spatial disposition of fluorenones rather that their amount [27,28]. According to this, the formation of fluorenone agglomerates is the cause for the increase of the green emission over the blue one during electro- (photo) oxidation. The reason for this is that when a fluorenone defect is formed, the alkyl chain is lost, favoring local interchain interaction between the PF backbone if several fluorenones are formed in spatial proximity on different PF chains. In this context, and based on our experimental results, we can inferred the following hypothesis to explain the less pronounced keto band in β-phase devices: the different morphology of the β-phase, in particular, the β-PFO chains adopting a planar zigzag structure which results in a longer conjugation length, may difficult the formation of fluorenone agglomerates. This does not mean that fluorenones cannot be formed, but they are spatially separated and hence, the effect of keto band in the EL spectra is less pronounced. In this context, devices containing a certain amount of β-phase show an ultrafast efficient energy transfer from the α- to the β-domains [29]. The minor presence of fluorenone agglomerates in the β-domain diminishes the green emission in the EL spectra. Therefore, a small percentage of β-phase in the PFO active layer results in higher color stability since it reduces the radiative transitions from the fluorenone sites. This result appears interesting to increase life time of PFO based PLEDs keeping high purity blue emission upon continuous operation.

In order to study electrical degradation mechanisms, *I–V* curves were measured and analyzed before and after subjecting the samples to electrical stressing. All *I–V* curves were examined using a single carrier conduction model that considers simultaneously both bulk transport and injection mechanisms. In this sense, the model does not assume previous simplifications such as injection limited (high injection barrier) or bulk limited (low mobility) conduction. Carrier transport in the bulk has been traditionally described in terms of Mott–Gurney formalism [30]. However, if a non-vanishing electric field at the interface (E_0) is present due to a non-negligible injection barrier, the integration of the electric field results in the *J–V* expression [20],

$$J_b(E_0,V_b)=\mu\varepsilon\varepsilon_0\frac{(9V_b^2-12E_0^2t^2)+\sqrt{(12E_0^2t^2-9V_b^2)^2-192\cdot E_0^3t^3(E_0t-V_b)}}{16\Phi t^3} \quad (1)$$

where J_b is the total current density in the bulk, V_b the applied voltage, μ is the dc equilibrium hole mobility, ε_0 is the vacuum permittivity, ε is the material dielectric constant, t is the sample thickness and Φ is the ratio between the carrier density actually contributing to transport and the total injected charge [31]. Notice that in the case of ohmic injection, E_0 vanishes and (1) reproduces the well known Mott–Gurney equation in the presence of carrier trapping,

$$J_{sc}=\frac{9}{8\Phi}\mu\varepsilon\varepsilon_0\frac{V_b^2}{t^3} \quad (2)$$

The total current across the diode can be obtained by numerically solving the continuity equation for the current at the anode interface,

$$J_{inj}(E_0)=J_b(V_b,E_0) \quad (3)$$

where J_{inj} is the injection current density at the anode interface. In this case, the injection mechanism chosen is that proposed by Arkhipov et al. [32]. This is based on a microscopic approach of carrier hopping between discrete states and involves a number of physical parameters such as: hole injection barrier, (Δ), and width of the Gaussian density of states, DOS, (σ). A detailed description of the total electrical model employed in this work can be found in previous works [20].

I–V curves for α- and β-PFO diodes were fitted using the above model before and after electrical degradation. Solid lines in Fig. 7 illustrate the fits.

Since the model is only valid for single carrier devices, simulations for non-degraded devices were carried out just before the onset of electroluminescence, that is, 100 μA and 500 μA for α- and β-phase respectively. Besides, at those current levels, degraded devices do not show emission.

The fitting procedure has been performed using a non-deterministic genetic algorithm. Solid lines in Fig. 7 show a reasonably good agreement between theory and experiment except for the degraded α-PFO diode. This can be attributed to the non-ideal behaviour introduced by leakage currents, that could be modelled in terms of circuital theory by introducing a parallel resistance.

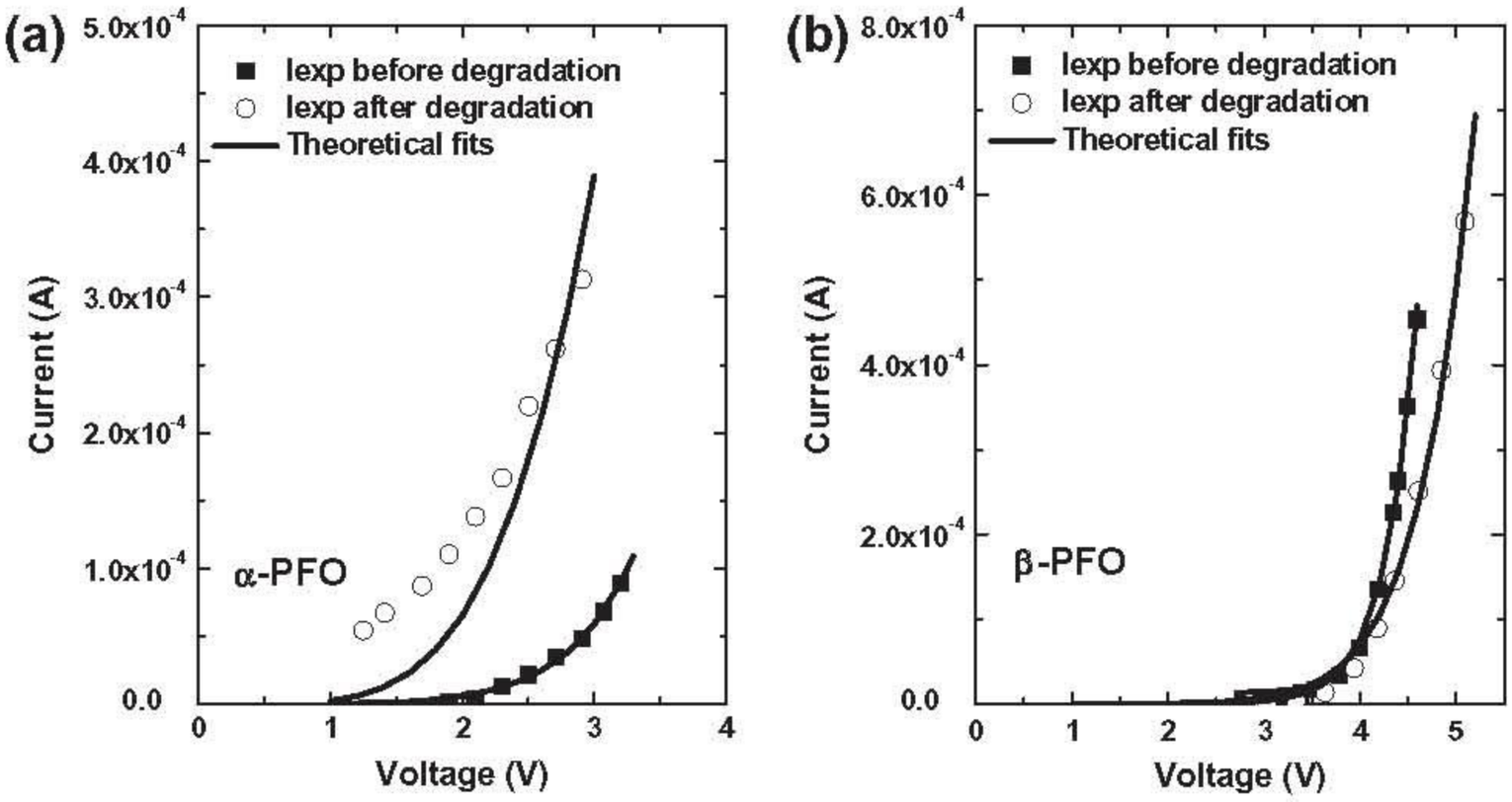

Fig. 7. Experimental *I–V* curves for α-PFO (a) and β-PFO (b) diodes. Curves were measured before (filled squares) and after (hollow circles) degradation. Theoretical fits are the solid lines. Simulations were performed for voltages below light-onset.

Table 1
Parameters obtained from the fits of Fig. 7. Effective mobility (μ^*), hole injection barrier (Δ), width of Gaussian density of states (σ).

	μ^* (cm^2/Vs)	Δ (eV)	σ (meV)
β-PFO diode before degradation	1.4×10^{-4}	0.47	44
β-PFO diode after degradation	7×10^{-6}	0.46	61
α-PFO diode before degradation	1.6×10^{-5}	0.47	40
α-PFO diode after degradation	9.2×10^{-7}	0.48	76

The set of physical parameters obtained from the fits are shown in Table 1.

Since carrier mobility is known to be dependent on both electric field and charge density [33,34], and moreover, not all the injected charge contributes to transport, μ^* must be considered as an average value within the range of applied voltages. Hole mobilities for pristine β- and α-PFO are in agreement with those values obtained using TOF techniques [35]. Furthermore, β-PFO mobility is about one order of magnitude higher than that of α-PFO, following the same tendency as that found using TOF [12]. The higher hole mobility for β-PFO is the result of the longer conjugation lengths of β-phase chains [6]. In the case of degraded β-PFO and α-PFO, the mobility decreases with respect to the pristine diodes by factors of 20 and 17 respectively. In addition, the model shows an increase of σ for both degraded PFO based diodes, indicating that the Gaussian Density of States broadens. Since charge transport occurs along localized states, an increase of the distribution width of localized states results in an increase of dispersive transport (that in turns appears as a consequence of hopping conduction in a disordered material). This is in agreement with a reduction of hole mobility, and thus, a worsening of charge transport. The resulting hole injection barrier is consistent with values found in literature of energy-level alignment between ITO/PEDOT work function and PFO HOMO level [36].

4. Conclusions

Analysis of the EL spectra along continuous operation time in α- and β-PFO based diodes reveals that the unwanted green emission traditionally associated to fluorenone is more likely to occur in α-phase PFO diodes. The different morphology of β-phase and its longer conjugation length may difficult the formation of fluorenone agglomerates, which is in agreement with recent studies that suggest that the unwanted green emission is more related to spatial disposition of fluorenones rather that their amount. Therefore, a small percentage of β-phase in the PFO active layer results in higher color stability since it reduces the radiative transitions from the fluorenone sites.

Study of the PLED *I–V* curve before and after undergoing electrical stressing reveals that effective hole mobility in pristine diodes is higher for β-PFO than for α-PFO as a result of the longer conjugation lengths of β-phase chains, being 1.4×10^{-4} and 1.6×10^{-5} cm^2/Vs respectively. Degraded diodes based on both α- and β-PFO show a reduction of hole mobility and an increase of the Gaussian Density of States width. This result suggests that the worsening of charge transport is related to an increase of disordered material and hence dispersive transport.

Acknowledgements

The authors would like to thank Drs. M. Clement, J. Olivares for thickness measurements. This work was supported by Comunidad Autónoma de Madrid under Projects S0505/ESP/0417 and S2009/ESP-1781, and by the Spanish Ministry of Education and Science under the Project TEC2006-13392-C02-02/MIC.

References

[1] Bernius M, Inbasekaran M, O'Brien J, Wu WS. Progress in light emitting polymers. Adv Mater 2000;12:1737.
[2] Bernius M, Inbasekaran M, Woo E, Wu W, Wujkowski L. Fluorene-based polymers-preparation and applications. J Mater Sci: Mater Electron 2000;11:111.
[3] Morgado J, Alcácer L, Charas A. Poly(9,9-dioctylfluorene)-based light-emitting diodes with pure β-phase emission. Appl Phys Lett 2007;90:201110.
[4] Misaki M, Chikamatsu M, Yoshida Y, Azumi R, Tanigaki N, Yase K, et al. Highly efficient polarized polymer light-emitting diodes utilizing oriented films of β-phase poly(9,9-dioctylfluorene). Appl Phys Lett 2008;93:023304.
[5] Arif M, Volz C, Guha S. Chain morphologies in semicrystalline polyfluorene: evidence from Raman scattering. Phys Rev Lett 2006;96:025503.
[6] Chunwaschirasiri W, Tanto B, Huber DL, Winokur MJ. Chain conformations and photoluminescence of poly(di-n-octylfluorene). Phys Rev Lett 2005;94:107402.
[7] Peet J, Brocker E, Xu Y, Bazan GC. Controlled β-phase formation in poly(9,9-di-n-octylfluorene) by processing with alkyl additives. Adv Mater 2008;20:1882.
[8] Ariu M, Sima M, Rahn MD, Hill J, Fox AM, Lidzey DG, et al. Exciton migration in β-phase poly(9,9-dioctylfluorene). Phys Rev B 2003;67:195333.
[9] Kasama D, Takata R, Kajii H, Ohmori Y. Optical property of poly(9,9-dioctylfluorene) gel with β phase and application to polymer light emitting diode. Thin Solid Films 2009;518:559.
[10] Ariu M, Lidzey DG, Sims M, Cadby AJ, Lane PA, Bradley DDC, et al. The effect of morphology on the temperature-dependent photoluminescence quantum efficiency of the conjugated polymer poly(9, 9-dioctylfluorene). J Phys: Condens Mater 2002;14:9975.
[11] Hayer A, Khan ALT, Friend RH, Kohler A. Morphology dependence of the triplet excited state formation and absorption in polyfluorene. Phys Rev B 2005;71:241302.
[12] Lu H-H, Liu C-Y, Chang C-H, Chen S-A. Self-dopant formation in poly(9,9-di-n-octylfluorene) via a dipping method for efficient and stable pure-blue electroluminescence. Adv Mater 2007;19:2574.
[13] Cadby AJ, Lane PA, Mellor H, Martin SJ, Grell M, Giebeler C, et al. Film morphology and photophysics of polyfluorene. Phys Rev B 2000;62:15604.
[14] Endo T, Kobayashi T, Nagase T, Naito H. Anisotropical optical properties of aligned β-phase polyfluorene thin films. Thin Solid Films 2008;517:1324.
[15] Chen SH, Su AC, Chen SA. Noncrystalline phases in poly(9,9-di-n-octyl-2,7-fluorene). J Phys Chem 2005;109:10067.
[16] Lee SK, Ahn T, Park J-H, Jung YK, Ching D-S, Park CE, et al. β-Phase formation in poly(9,9-di-n-octylfluorene) by incorporating an ambipolar unit containing phenothiazine and 4-(dicyanomethylene)-2-methyl-6-[p-(dimethylamino)-styryl]-4H-pyran. J Mater Chem 2009;19:7062.
[17] Dias FB, Morgado J, Macanita AL, da Costa FP, Burrows HD, Monkman AP, et al. Kinetics and thermodynamics of poly(9,9-dioctylfluorene) β-phase formation in dilute solution. Macromolecules 2006;39:5854.
[18] Kitts C, Vanden Bout DA. The effect of solvent quality on the chain morphology in solutions of poly(9,90-dioctylfluorene). Polymer 2007;48:2322.
[19] Romero B, Arredondo B, Alvarez AL, Mallavia R, Salinas A, Quintana BX, et al. Influence of electrical operating conditions and active layer thickness on electroluminescence degradation in polyfluorene-phenylene based light emitting diodes. Solid-State Electron 2009;53:211.
[20] Alvarez AL, Arredondo B, Romero B, Gutiérrez-Llorente A, Quintana X, Mallavia R, et al. Analytical evaluation of the ratio between injection and space-charge limited currents in single carrier organic diodes. IEEE Trans Electron Dev 2008;55:674.
[21] Gaal M, List EJW, Scherf U. Excimer or emissive on – chain defects? Macromolecules 2003;36:1750.
[22] Romaner L, Pogantsch A, de Freitas PS, Gaal M, Zojer E, List EJW. The origin of green emission in polyfluorene-based conjugated polymers: on-chain defect fluorescence. Adv Funct Mater 2003;13:597.
[23] Gamerith S, Gadermaier C, Scherf U, List EJW. Emission properties of pristine and oxidatively degraded polyfluorene type polymers. Phys Status Solidi A: Appl Res 2004;201:1132.
[24] Dias FB, Knaapila M, Monkman AP, Burrows HD. Fast and slow time regimes of fluorescence quenching in conjugated polyfluorene–fluorenone random copolymers: the role of exciton hopping and dexter transfer along the polymer backbone. Macromolecules 2006;39:1598.
[25] Zhou X-H, Zhang Y, Xie Y-Q, Cao Y, Pei J. Effect of fluorenone units on the property of polyfluorene and oligofluorene derivatives: synthesis structure–properties relationship and electroluminescence. Macromolecules 2006;39:3830.
[26] Montilla F, Mallavia R. On the origin of green emission bands in fluorene-based conjugated polymers. Adv Func Mater 2007;17:71.
[27] Grisorio R, Suranna GP, Mastrorilli P, Nobile CF. Insight into the role of oxidation in the thermally induced green band in fluorene-based systems. Adv Funct Mater 2007;17:538.
[28] Kim YH, Vanden Bout DA. The effects of photochemical oxidation and chain conformation on green emission of poly(9,9-dioctylfluorene). Appl Phys A 2009;95:241.
[29] Hayer A, Khan ALT, Friend RH, Köhler A. Morphology dependence of the triplet excited state formation and absorption in polyfluorene. Phys Rev B 2005;71:241302.

[30] Mott NF, Gurney RW. Electronic process in ionic crystals. 2nd ed. Oxford University Press; 1948.
[31] Arkhipov VI, von Seggern H, Emelianova EV. Charge injection versus space-charge-limited current in organic light emitting diodes. Appl Phys Lett 2003;83:5074.
[32] Arkhipov VI, Emelianova EV, Taknad YH, Bässler H. Charge injection into light-emitting diodes: theory and experiment. J Appl Phys 1998;84: 848.
[33] F Pasveer W, Cottaar J, Tanase C, Coehoorn R, Bobbert PA, Blom PWM, et al. Unified description of charge-carrier mobilities in disordered semiconducting polymers. Phys Rev Lett 2005;94:206601.
[34] Bisquert J, Montero JM, Bolink HJ, Barea EM, Garcia-Belmonte G. Thickness scaling of space-charge-limited currents in organic layers with field- or density-dependent mobility. Phys State Solid A 2006;203:3762.
[35] Kreouzis T, Poplavskyy D, Tuladhar SM, Campoy-Quiles M, Nelson J, Campbell AJ, et al. Temperature and field dependence of hole mobility in poly(9,9-dioctylfluorene). Phys Rev B 2006;73:235201.
[36] Ryu Seung Yoon, Kim Jong Tae, Noh Joo Hyon, Hwang Byoung Har, Kim Chang Su, Jo Sung Jin, et al. Polymeric tandem organic light-emitting diodes using a self-organized interfacial layer. Appl Phys Lett 2008;92:103301.